DNR-239

Project Final Report

Investigation of PFAS adsorption by selected Wisconsin aquifer sediments

Prepared by:

Yin Wang
Department of Civil and Environmental Engineering
University of Wisconsin – Milwaukee

Shangping Xu
Department of Geosciences
University of Wisconsin – Milwaukee

Table of Contents

List of Tables

List of Figures

Keywords

PFAS; Adsorption; Aquifer material; Groundwater; Dolomite; Transport

Acknowledgements

The experimental work described in this report was supported by the Wisconsin Department of Natural Resources (DNR Proj# 239). Graduate students on this project included Yanan Zhao, Brittany Grosskopf, and Zachary Henderson at the University of Wisconsin – Milwaukee. We are grateful to Dr. Matthew Silver and the DNR support team for their help and guidance during the project.

Project Summary

Title: Investigation of PFAS adsorption by selected Wisconsin aquifer sediments

Project I.D.: DNR-239

Investigators: Yin Wang (PI), Associate Professor, Department of Civil and Environmental Engineering, University of Wisconsin – Milwaukee

Shangping Xu (Co-PI), Associate Professor, Department of Geosciences, University of Wisconsin – Milwaukee

Period of Contract: July 1, 2020 – June 30, 2022

Background: Per- and polyfluoroalkyl substances (PFAS) are a large class of synthetic organic chemicals that are widely used in a variety of applications. Due to their diverse structure and widespread use, PFAS have been detected in waterways across the U.S. As human exposure to PFAS has been linked to cancer, elevated cholesterol, obesity, immune suppression, and endocrine disruption, the occurrence of PFAS in the natural environment is raising public health concerns. Specifically, PFAS contamination has been reported in numerous Wisconsin groundwater aquifers. Since PFAS tend to be stable in the natural environment, the transport and fate of PFAS within the groundwater system is directly related to their adsorption onto the aquifer materials which in turn is strongly dependent on the compositions and properties of the aquifer materials. As a result, site-specific investigation would be required to reliably predict the subsurface transport of PFAS. To the best of our knowledge, however, the adsorption of PFAS onto aquifer materials relevant to Wisconsin aquifer settings has remained largely unexplored.

Objectives: The overall objective of this project was to investigate the adsorption behavior of PFAS onto several representative Wisconsin aquifer materials collected from sites susceptible to PFAS contamination. The sites were selected for their geographical coverage, their different aquifer material composition, and their proximity to known and possible PFAS sources. Our central hypothesis was that PFAS adsorption onto aquifer materials would depend on both PFAS structure and aquifer material composition, and longer-chain PFAS would show stronger adsorption affinity with aquifer materials than those of shorter-chain PFAS.

Methods: Aquifer materials of varied compositions were collected from five representative locations across Wisconsin in the counties of Dane, La Crosse, Marinette, Waukesha, and Washington. For comparison purpose, dolomite samples were also collected from a quarry located in Sussex, WI and was ground to granules before use. Six representative PFAS with different carbon chain lengths and end functional groups were selected for investigation, including perfluorooctanesulfonic acid (PFOS), perfluorooctanoic acid (PFOA), perfluorononanoic acid (PFNA), perfluoroheptanoic acid (PFHpA), perfluorohexanesulfonic acid (PFHxS), and perfluorobutanesulfonic acid (PFBS). Detailed adsorption isotherm experiments were performed to determine the aquifer material-water partition coefficients (K_d) of PFAS. Specifically, experiments were conducted with the six PFAS mixture in a representative groundwater matrix and a range of environmentally relevant concentrations (nominally 100 – 5000 ng/L for each PFAS). Furthermore, the measured K_d values were applied to a one-dimensional (1-D) transport model to illustrate the impact of PFAS adsorption on PFAS transport in groundwater aquifer.

Results and Discussion: Aquifer materials mainly consisted of dolomite ($CaMg(CO_3)_2$) and/or quartz (SiO_2), and the relative abundance of the two minerals were substantially varied among

different aquifer materials. In general, PFAS adsorption onto aquifer materials could be described by the linear isotherm model, suggesting the relatively constant adsorption affinity between PFAS and aquifer materials under environmentally relevant conditions. PFAS adsorption was highly dependent on aquifer material composition, particularly dolomite content. Aquifer materials of higher dolomite content showed significantly stronger affinity with PFAS than those of lower dolomite content. Compared to dolomite content, other parameters of aquifer material such as contents of SiO_2, Al, and Fe, cation exchange capacity (CEC), anion exchange capacity (AEC), and porosity played a less substantial role in PFAS adsorption. Furthermore, PFAS adsorption was also strongly related to PFAS structure. Longer-chain PFAS had higher adsorption affinity with aquifer materials than those of shorter-chain PFAS, and perfluorinated sulfonic acids were more strongly adsorbed onto aquifer materials than perfluorinated carboxylic acids. Octanol-water distribution coefficient (D_{ow}) could be considered a good indicator to correlate PFAS structure with their adsorption onto aquifer materials. An empirical model was established based on multilinear regression of the experimental data to determine $log\ K_d$ of PFAS onto aquifer materials based on dolomite content of aquifer material and $log\ D_{ow}$ of PFAS.

Conclusions and Implications: This project suggested that dolomite played an important role in PFAS adsorption onto aquifer materials. Aquifer materials with high dolomite content may show more significant retention of PFAS and stronger retardation on PFAS transport in comparison to materials with low dolomite content, and thus reduce the likelihood and extent of PFAS contamination of the groundwater. It is worth mentioning that while this project primarily investigated the adsorption of six representative PFAS, the adsorption affinity of other relevant anionic PFAS onto aquifer materials may be readily predicted based on their $log\ D_{ow}$ values. The fundamental information obtained from this project can help provide a quantitative understanding of the fate and transport potential of PFAS in impacted groundwater aquifers in Wisconsin, which can be used to develop improved strategies for remediation of PFAS-contaminated sites, and guide general PFAS management practices in groundwater in Wisconsin. Considering the complexity of aquifer settings, combined experimental and modeling efforts are recommended to improve the understanding of PFAS adsorption and transport behavior in various complex aquifer systems.

Related Publications/Presentations:

Zhao Y., Min X., Xu S., Wang Y. Adsorption of per- and polyfluoroalkyl substances by aquifer materials: the important role of dolomite. *Environmental Science & Technology Letters*, **2023**, 10, 931-936, DOI: 10.1021/acs.estlett.3c00583

Zhao Y., Grosskopf B.C., Min X., Henderson Z.D., Xu S., Wang Y. Adsorption of PFAS by aquifer materials: Implications on PFAS transport in groundwater. 265th American Chemical Society National Meeting, March 26-30, **2023**, Indianapolis, IN and online.

Zhao Y., Grosskopf B.C., Min X., Henderson Z.D., Xu S., Wang Y. Investigation of PFAS adsorption onto aquifer materials in Wisconsin. Wisconsin AWRA 2023 Annual Meeting, March 16-17, **2023**, Wisconsin Dells, Wisconsin.

Zhao Y., Grosskopf B.C., Min X., Henderson Z.D., Xu S., Wang Y. Adsorption of perfluoroalkyl acids onto aquifer materials with varied composition. The 2023 Emerging Contaminants in the Environment Conference (ECEC23), April 18-19, **2023**, Champaign, IL and online.

Key Words: PFAS; Adsorption; Aquifer material; Groundwater; Dolomite; Transport

Funding: Wisconsin Department of Natural Resources

Objective

Per- and polyfluoroalkyl substances (PFAS) are a large class of emerging pollutants that have been widely detected in both natural and engineered aquatic systems in the United States, including Wisconsin groundwater aquifers. Transport of PFAS in groundwater is strongly affected by their adsorption onto the aquifer materials, and thus detailed and site-specific investigation on PFAS adsorption behavior would be required to reliably predict the transport of PFAS at an impacted site. The **overall objective** of this project was to investigate the adsorption behavior of PFAS onto several representative Wisconsin aquifer materials collected from sites susceptible to PFAS contamination. The sites were selected for their geographical coverage, their different aquifer material composition, and their proximity to known and possible PFAS sources. Our central **hypothesis** was that PFAS adsorption onto aquifer materials would depend on both PFAS structure and aquifer material composition, and longer-chain PFAS would show stronger adsorption affinity with aquifer materials than those of shorter-chain PFAS.

Background

PFAS are a large class of synthetic organic chemicals that have been widely used since 1940s in a variety of applications, such as surface coatings, production of fluoropolymers, surfactants, and firefighting foams [1]. It was estimated that several thousand PFAS compounds have been used in different formulations on the global markets [2]. Because of the perfluoroalkyl moiety ($C_nF_{2n+1}-$), PFAS have a series of unique properties, such as strong acidity, high stability, and improved surface activity at low concentrations [3]. Particularly, many PFAS are very persistent in the natural environment and they are generally recalcitrant to biological and chemical decomposition, due to the strong carbon-fluorine bond [4]. Although some PFAS may partially degrade in the environment, they may ultimately transform into the highly stable end products, such as perfluoroalkyl acids (PFAAs), which are highly soluble in water under ambient pH conditions [5]. Human exposure to PFAS has been linked to cancer, elevated cholesterol, obesity, immune suppression, and endocrine disruption [6]. Perfluorooctanesulfonic acid (PFOS) and perfluorooctanoic acid (PFOA) are two legacy PFAS that have drawn most attention in the scientific and regulation communities [5]. PFOS, PFOA, as well as their precursors, are currently listed under the Stockholm Convention on Persistent Organic Pollutants [7].

As a result of their widespread use, the detection of PFAS have been documented across the globe [8, 9]. For instance, Gobelius et al reported the detection of PFAS in >90% of the samples collected in Swedish groundwater and surface water [10]. In the U.S., PFAS have been found in the public water supplies in 33 states, based on the spatial analysis of data collected from the U.S. EPA's third Unregulated Contaminant Monitoring Rule (UCMR3) [11]. The USEPA's fifth Unregulated Contaminant Monitoring Rule (UCMR5) further required the public water systems in the U.S. to monitor 29 PFAS between 2023 and 2025 [12]. Elevated PFAS concentrations have been reported in drinking water sources in many regions near the industrial sites that produce or use these compounds [13, 14]. Military fire training areas and civilian airports are another major source of PFAS contamination because of the use of aqueous film-forming foams (AFFFs) during firefighting training activities [15, 16]. PFAS concentrations that are several orders of magnitude higher than the U.S. EPA health advisory have been reported in groundwater surrounding these sites [17, 18]. Other important PFAS sources include wastewater treatment plants (i.e., PFAS

cannot be removed by standard treatment methods) and landfill [19-21]. The widespread presence of PFAS in the environment, along with their known adverse effects on human health, has caused growing concern among the public [22].

PFAS contamination has been found in numerous Wisconsin groundwater aquifers [23]. For example, high PFOS and PFOA concentrations have been reported in groundwater wells in Marinette, WI that is home of a fire products manufacturing plant, and it is estimated that over $100 million would be required for the cleanup of the PFAS contaminated sites [24]. Elevated PFOS and PFOA concentrations have also been observed in groundwater near a military site at Milwaukee, WI [25]. Additionally, the water utility at Madison, WI reported the detection of PFAS in 14 of the city wells [26]. PFAS have also been found in two city wells close to a civilian airport at La Crosse, WI [27]. Due to the rising concern of PFAS contamination in Wisconsin, the Wisconsin PFAS Action Council developed the Wisconsin PFAS Action Plan in 2020, which served as the roadmap to address PFAS-related issues in Wisconsin [28]. The Wisconsin Department of Health Services (DHS) has recommended a health-based groundwater standard for 18 PFAS including PFOS and PFOA. Further, Wisconsin has established maximum contaminant levels (MCLs) of 70 ng/L for PFOS and PFOA, individually and combined, in public drinking water [29]. Groundwater is a major drinking water source in Wisconsin that it serves about two thirds of Wisconsin's population. Therefore, an improved understanding of PFAS transport in groundwater aquifers, especially in those high-risk areas, would be greatly beneficial for the development of PFAS management and remediation strategies to protect public health.

The transport and fate of PFAS in groundwater strongly depends on their interaction with the aquifer materials. Numerous studies have investigated the adsorption of PFAS onto natural materials including soils, sediments, and minerals, and results have suggested that binding of PFAS with natural materials can be affected by many factors, such as the composition and property of materials, the structure and functionality of PFAS, and the water chemistry condition [30-33]. It has been suggested that organic matter played an important role in PFAS adsorption onto natural materials. For instance, Higgins and Luthy found that sediments with relatively high organic carbon contents tended to have stronger interaction with longer-chained PFAS, and the sorption of PFAS to sediment increased for each CF_2 moiety by 0.5 – 0.6 log units of the measured partition coefficients, probably due to the enhanced hydrophobic interaction [34]. Compared to soils and sediments, aquifer materials generally contain low organic carbon contents, and thus PFAS adsorption is primarily governed by their interactions with the mineral phases within aquifer materials. Dolomite is commonly present in aquifer materials and is considered the predominant mineral in dolomite aquifers. However, the interaction between PFAS and dolomite has been historically overlooked. Furthermore, because of the complex interactions between PFAS and aquifer materials, detailed and site-specific investigation on PFAS adsorption behavior would be needed to reliably predict the subsurface transport of PFAS at an impacted site. However, to the best of our knowledge, the adsorption of PFAS onto aquifer materials relevant to Wisconsin aquifer settings has remained largely unexplored.

Materials and Methods

Chemicals

This project examined six representative PFAAs with different carbon chain lengths and end functional groups, including PFOS (98%, Sigma-Aldrich), PFOA (95%, Alfa Aesar), perfluorononanoic acid (PFNA, Sigma-Aldrich, 97%), perfluoroheptanoic acid (PFHpA, Sigma-Aldrich, 99%), perfluorohexanesulfonic acid in potassium salt (PFHxS, Sigma-Aldrich, 98%), and perfluorobutanesulfonic acid (PFBS, Sigma-Aldrich, 97%). These PFAS were listed both in the U.S. EPA's UCMR3 and UCMR5, and were selected based on their environmental relevance and persistent nature. **Table 1** showed the chemical structures and main physicochemical parameters of the selected PFAS. Mass-labelled standards solutions of the six PFAS were purchased from Wellington Laboratories and used as internal standards.

Table 1. Chemical structure and physiochemical properties of PFAS examined in this study.

PFAS	Chemical Structure	Molecular Weight (g/mol)	CMC (mM) [a]	Log K_{ow} [b]	Log D_{ow} at pH 8.5 [b]
PFBS	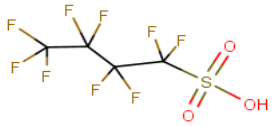	300.1	22	2.63	0.25
PFHpA		364.06	33	4.41	0.88
PFOA	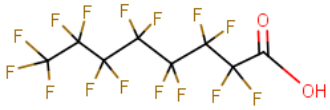	414.07	9	5.11	1.58
PFHxS	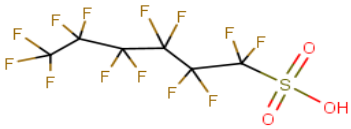	400.12	12	4.03	1.65
PFNA	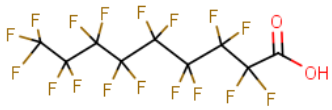	464.08	3.1	5.81	2.28
PFOS	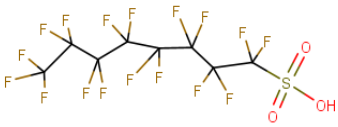	500.13	3.1	5.43	3.05

[a] CMC (critical micelle concentration) values were obtained from reference [32].

[b] Log K_{ow} (octanol-water partition coefficient) and Log D_{ow} (octanol-water distribution coefficient) at pH 8.5 were obtained from MarvinSketch 22.13, which were estimated based on PFAS structure.

Aquifer material selection and characterization.

Aquifer materials used in this study were collected from five representative locations across Wisconsin in the counties of Dane, La Crosse, Marinette, Waukesha, and Washington (**Figure 1**, #1 – 5). For comparison purpose, dolomite samples were also collected from a quarry located in Sussex, WI (#6) and were ground to granules before use. Briefly, there are four main aquifers within Wisconsin and the aquifers are layered in varying thicknesses, one atop another. On the surface lies the sand and gravel aquifer, which is neither distributed uniformly across the state nor is continuous over large areas. The sand and gravel aquifer are commonly used for water supply purposes but is particularly vulnerable to contamination from surface pollutants. The dolomite aquifer is primarily located within the eastern part of Wisconsin along the shoreline of Lake Michigan. The sandstone aquifer lies at the surface in southwestern Wisconsin, beneath the sand and gravel aquifer in central Wisconsin and beneath the dolomite aquifer (as well as the shale aquitard) in eastern Wisconsin. The crystalline bedrock is generally overlain by sandstone, dolomite, or glacial deposits. The crystalline bedrock aquifer represents a major water source only in north central Wisconsin. The aquifer materials used in this research, with a reasonable geographic coverage of the state, were collected below the water table during well drilling projects. Prior to the adsorption experiments, the aquifer materials were cleaned with methanol and deionized (DI) water to remove any possible background PFAS accumulated within the materials [35, 36]. The cleaned aquifer materials were oven dried at 105 °C, sieved with 2 mm sieve, and preserved for use.

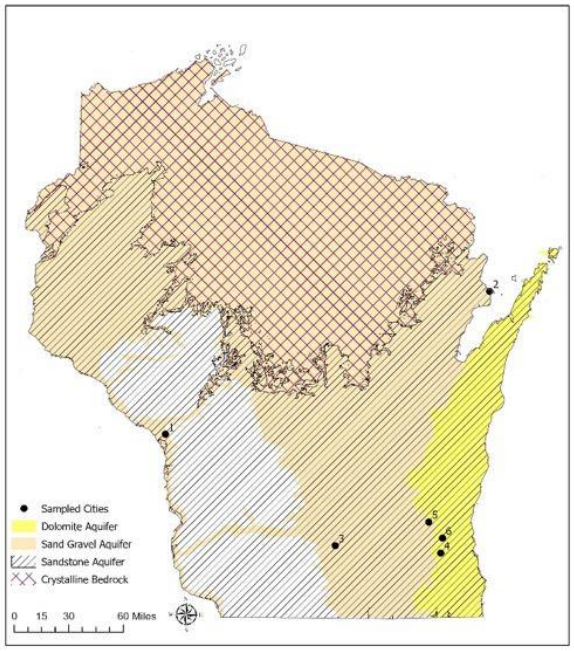

Figure 1. Map of the aquifer material collection sites and the four main aquifers within Wisconsin.

The crystalline phases of the aquifer materials were characterized by powder X-Ray diffraction (XRD) with a Bruker D8 Discover A25 diffractometer with copper Kα radiation. Fourier-transform infrared spectroscopy (FTIR) was used to investigate the surface functional groups of the aquifer materials with a Shimadzu IRTracer100 Spectrometer. The vibrations corresponding to the wavenumbers in the range of 400–4000 cm^{-1} were collected with a resolution of 4 cm^{-1}.

Zeta potentials of the aquifer materials were measured with a Malvern Zeta sizer Nano ZS 90. The pH, bulk density, porosity, cation exchange capacity (CEC), and anion exchange capacity (AEC) of the aquifer materials were determined using standard methods [34, 37, 38]. The total organic carbon (TOC) content of the aquifer materials was determined on a NA 1500 NCS combustion analyzer (Carlo Erba instruments) after acid pretreatment to remove inorganic carbonates [39, 40]. The carbon contents of the aquifer materials prior to and after acid pretreatment were used to estimate the concentrations of inorganic carbonates within the aquifer materials. Elemental composition of the aquifer materials was determined with X-ray fluorescence (XRF, Bruker AXS S4 pioneer).

Batch adsorption experiments and PFAS analysis.

Batch adsorption isotherm experiments were performed to determine the adsorption behavior of PFAS onto the aquifer materials. Experiments were conducted in polypropylene tubes at room temperature (22±2 °C) with a fixed aquifer material loading of 100 g/L under a representative groundwater matrix. The groundwater was collected from a drinking water supply well in Wisconsin, and was filtered with 0.2 µm polyether-sulfone (PES) membrane prior to experiments. The groundwater had a pH of 8.5 with moderate levels of hardness and dissolved organic carbon (DOC) of 155 mg/L as $CaCO_3$ and 1.2 mg/L as C, respectively. A mixture of the six PFAS was spiked to the groundwater to produce a series of environmentally relevant initial concentrations (nominally 100 – 5000 ng/L for each PFAS). After 7 days of contact time on a shaker, the solution was separated from aquifer material through centrifugation. The collected supernatant was immediately diluted with methanol in a 1:1 ratio, and an aliquot of acetic acid (0.1%) was added to adjust the pH to 3 – 4 to enhance PFAS measurement sensitivity. Concentrations of the six PFAS mixture were quantified on ultra-high-performance liquid chromatography (UHPLC, Shimadzu Nexera X2) coupled with ultra-fast triple quadrupole mass spectrometry (UFMS, Shimadzu LCMS-8060) through the isotope dilution method with the use of the mass-labeled six PFAS mixture as internal standards (**Table 2**). The detailed PFAS analytical method can be found in Appendix.

Table 2. MS/MS conditions and detection limits for the six PFAS using LC-MS/MS.

Analyte	Precursor ion (m/z)	Product ion (m/z)	Collision energy (V)	Internal standard
PFBS	299.1	80.1	36.0	M3PFBS
PFHpA	363.0	319.0	10.0	M4PFHpA
PFOA	413.0	369.0	11.0	M8PFOA
PFHxS	399.0	80.0	42.0	M3PFHxS
PFNA	463.0	418.9	10.0	M9PFNA
PFOS	498.9	80.0	55.0	M8PFOS

The PFAS adsorption amount was calculated with Equation 1.

$$Q_e = \frac{(C_0 - C_e) \cdot V}{M} \quad (1)$$

where Q_e (ng/g) presents the amount of PFAS adsorbed on aquifer materials at equilibrium, C_0 (ng/L) and C_e (ng/L) represent the initial and equilibrium PFAS concentrations, respectively, V (L) is PFAS solution volume, and M (g) is the aquifer materials mass.

One-dimensional transport modeling development

The measured adsorption parameters were applied to a one-dimensional (1-D) transport model to illustrate the impact of PFAS adsorption on PFAS transport in groundwater. Due to the slow velocity of groundwater flow, it is reasonable to assume that the adsorption of PFAS onto the aquifer materials is at equilibrium:

$$S = K_d C \tag{2}$$

where C (ng/L) is the pore water concentration of PFAS; S (ng/kg) is the concentration of adsorbed PFAS, and K_d (L/kg) is the distribution coefficient. Under the presence of equilibrium adsorption, the transport of PFAS within the aquifer materials can be described by the following mass balance equation [41, 42]:

$$\frac{\partial C}{\partial t} = -v\frac{\partial C}{\partial x} + D\frac{\partial^2 C}{\partial x^2} - \frac{\rho}{\theta}\frac{\partial S}{\partial t} \tag{3}$$

where t (s) is time; v (m/s) is the average linear pore water velocity; x (m) is the coordinate parallel to flow; and D (m^2/s) is the hydrodynamic dispersion coefficient; ρ (kg/L) is the bulk density of aquifer material and θ is the porosity of the aquifer material.

Substituting Equation 2 into Equation 3, we have

$$\frac{\partial C}{\partial t} = -v\frac{\partial C}{\partial x} + D\frac{\partial^2 C}{\partial x^2} - K_d\frac{\rho}{\theta}\frac{\partial C}{\partial t} \tag{4}$$

$$\left(1 + K_d\frac{\rho}{\theta}\right)\frac{\partial C}{\partial t} = -v\frac{\partial C}{\partial x} + D\frac{\partial^2 C}{\partial x^2} \tag{5}$$

The term $\left(1 + K_d\frac{\rho}{\theta}\right)$ is unitless and is often referred to as the retardation factor R [41]:

$$R\frac{\partial C}{\partial t} = -v\frac{\partial C}{\partial x} + D\frac{\partial^2 C}{\partial x^2} \tag{6}$$

$$\frac{\partial C}{\partial t} = -\frac{v}{R}\frac{\partial C}{\partial x} + \frac{D}{R}\frac{\partial^2 C}{\partial x^2} \tag{7}$$

For illustration purposes, we assumed that the source of contamination was continuous. Thus, Equation 7 can be solved analytically and the corresponding solution (for contaminant aqueous concentration C as a function of travel distance x and time t) is [41]:

$$C = \frac{C_0}{2}\operatorname{erfc}\left[\frac{Rx - vt}{2\sqrt{DRt}}\right] + \frac{C_0}{2}e^{\frac{vx}{D}}\operatorname{erfc}\left[\frac{Rx + vt}{2\sqrt{DRt}}\right] \tag{8}$$

where erfc() represents the complementary error function. Equation 8 allows us to compare the transport of different PFAS within the subsurface under the presence of different adsorption behavior.

Results and Discussion

Characterization of aquifer materials

The structural, compositional, and physicochemical properties of the aquifer materials were extensively characterized. Dolomite ($CaMg(CO_3)_2$) and/or quartz (SiO_2) were identified as the main minerals of the aquifer materials, evidenced by the peaks at 2θ of 26.6° and 30.9° that were characteristic of quartz and dolomite, respectively, from the XRD patterns (**Figure 2a**). Meanwhile, the relative abundance of the two minerals were quite different among different aquifer materials, based on their different relative peak intensities. Although aquifer material #6 was collected from a dolomite rock, quartz was observed as a minor phase within that material. The presence of dolomite and/or quartz was further confirmed based on FTIR measurement. As shown in **Figure 2b**, the peaks at 715-725 cm^{-1}, 870-880 cm^{-1}, and 1410 - 1460cm^{-1} were assigned to C=O band, O-C-O bending, and CO_3^{2-} stretching of dolomite, respectively. Meanwhile, the peaks at 770 - 780 cm^{-1} and 1040 - 1070 cm^{-1} were related to Si–O symmetrical stretching vibration and SiO deformation band, respectively [43-45]. Based on carbon elemental analysis and the stoichiometry of dolomite, dolomite contents within the aquifer materials were determined and followed the trend that aquifer material #1 < #2 ≈ #3 < #4 < #5 < #6 (**Table 3**). As expected, all aquifer materials had negligible organic carbon contents, since they were collected more than 70 ft below ground surface (BGS). XRF analysis suggested that Ca, Mg, and/or Si were the major elements of the aquifer materials (**Table 4**), which were consistent with the XRD and FTIR findings of dolomite and/or quartz as main minerals. Additionally, Al, Fe, and Na were observed as minor elements of the aquifer materials. It was worth mentioning that the loss-on-ignition (LOI) data of XRF matched quite well with the carbon elemental analysis results, which was attributed to the decomposition of carbonates to CO_2. Zeta potential measurements suggested that all aquifer materials carried negative surface charges under circumneutral conditions (**Table 3**).

Table 3. Selected properties of aquifer materials examined in this project.

Aquifer material	pH	Bulk density (g/cm^3)	Porosity	TOC (wt%)	CEC (μeq/g)	AEC (μeq/g)	Zeta potential at pH 7 (mV)	Dolomite content (wt%)
#1	8.39	1.66	0.33	< 0.1	22.48	0.07	-21.8	1.8
#2	8.54	1.75	0.33	< 0.1	11.09	0.17	-11.7	17.9
#3	8.49	1.75	0.35	< 0.1	37.17	0.12	-19.2	20.6
#4	8.40	1.62	0.40	< 0.1	29.40	0.65	-11.0	48.4
#5	8.90	1.91	0.27	< 0.1	48.89	0.43	-18.5	63.2
#6	9.20	1.88	0.32	< 0.1	31.20	0.14	-12.8	86.6

Table 4. Composition of aquifer materials based on XRF analysis.

	Aquifer Material					
	#1	**#2**	**#3**	**#4**	**#5**	**#6**
Na_2O	0.93%	0.59%	0.30%	0.39%	0.25%	ND [a]
MgO	0.70%	3.27%	4.61%	10.42%	13.02%	18.90%
Al_2O_3	4.86%	4.75%	2.85%	3.16%	2.96%	0.98%
SiO_2	89.71%	73.87%	75.03%	43.70%	31.63%	13.88%
K_2O	1.19%	1.96%	0.88%	0.84%	0.89%	0.24%
CaO	1.40%	6.82%	6.88%	17.66%	21.70%	28.12%
Fe_2O_3	1.34%	1.35%	0.98%	1.33%	1.35%	0.24%
LOI	0.94%	8.31%	8.88%	21.70%	31.44%	41.77%

[a] ND: not detected

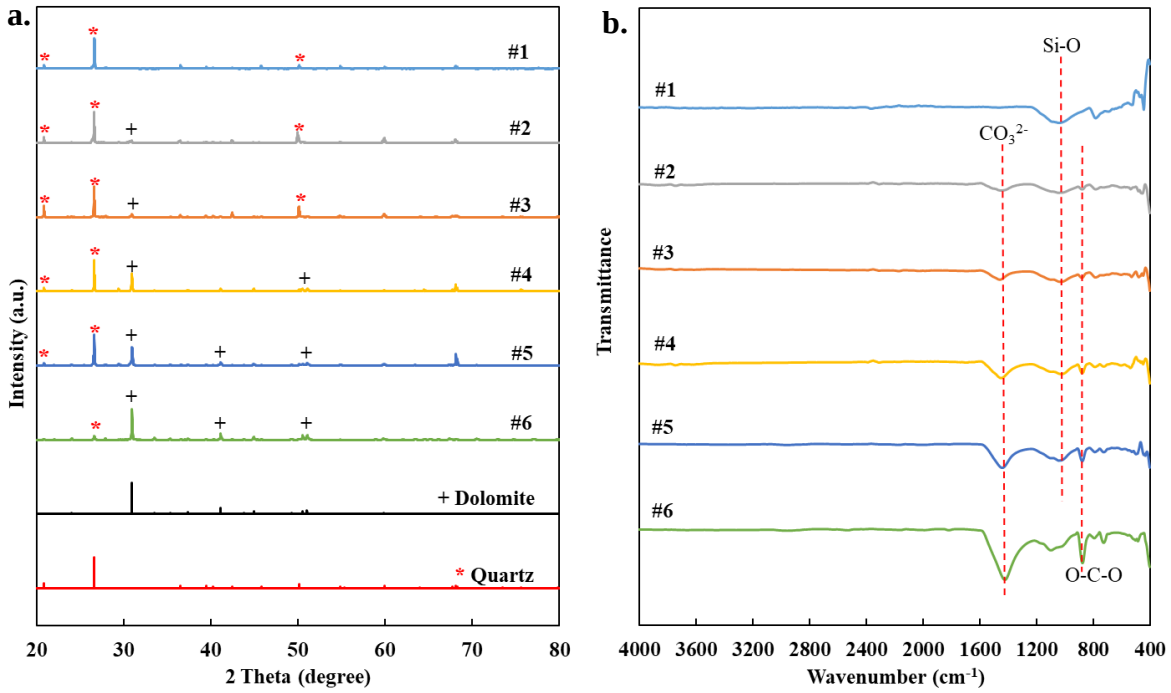

Figure 2. (**a**) XRD patterns and (**b**) FTIR spectra of the aquifer materials. The reference patterns of dolomite (PDF #00-036-0426) and quartz (PDF #00-046-1045) are also shown in panel (a) for comparison.

PFAS adsorption behavior onto aquifer materials

To investigate PFAS adsorption behavior onto aquifer materials, we performed isotherm studies of a mixture of six selected PFAAs under a range of environmentally relevant concentrations and

a representative groundwater matrix (**Figure 3**). All adsorption isotherms could be adequately fitted with the linear isotherm model (Equation 9) under the experimental condition.

$$Q_e = K \cdot C_e \tag{9}$$

where K (L/g) is the linear adsorption constant, and Q_e (ng/g) and C_e (ng/L) had the same meanings as those in Equation 1. Based on the linear adsorption isotherm, the aquifer material-water partition coefficients (K_d, L/kg) could be determined using Equation 10:

$$K_d = \frac{Q_e}{C_e} = K \cdot 1000 \tag{10}$$

where 1000 is a unit conversion factor between kg and g. The linear isotherm fitting parameters as well as the corresponding K_d values were shown in **Table 5**.

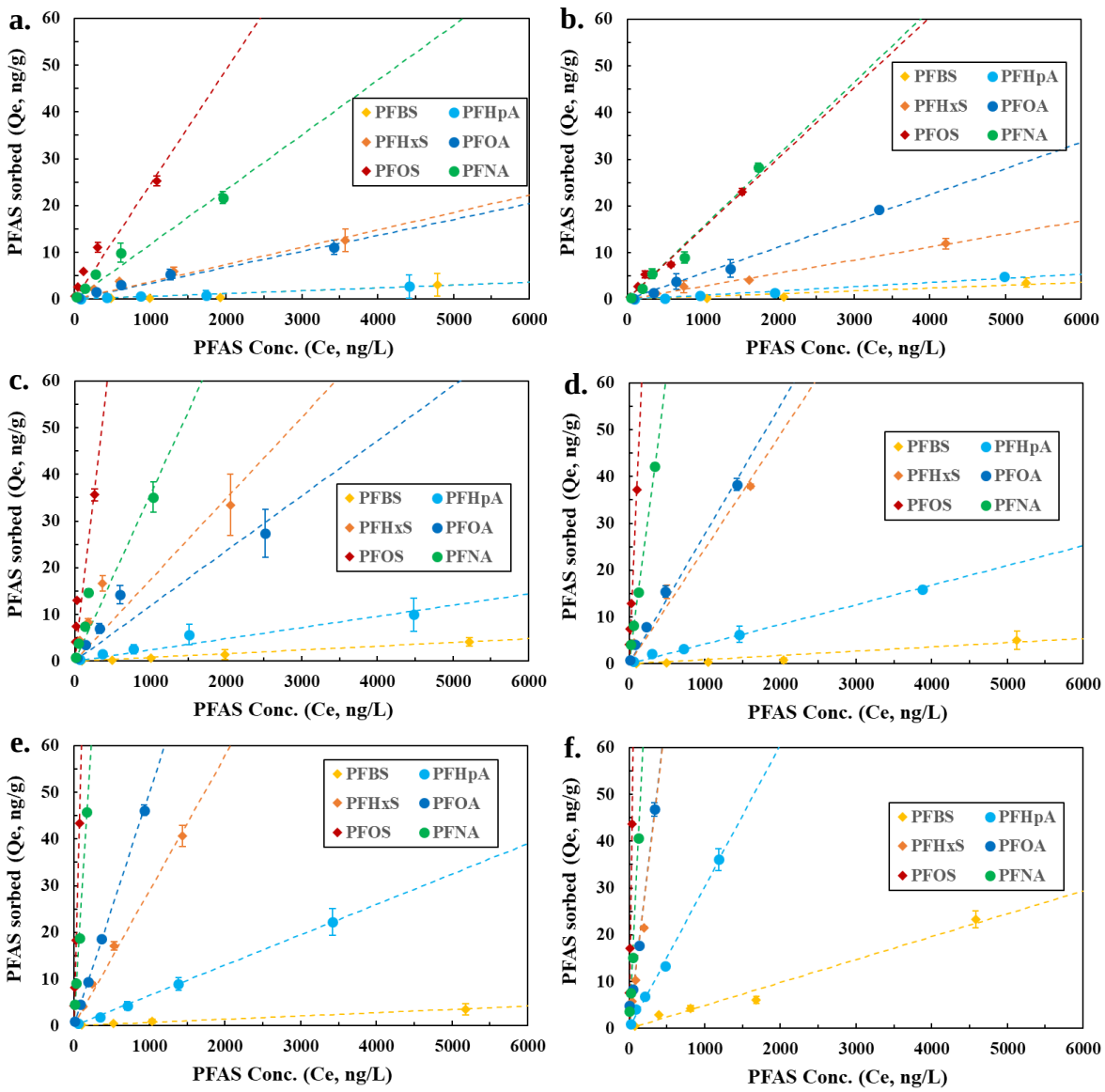

Figure 3. Adsorption isotherms of PFAS onto aquifer materials (**a**) #1, (**b**) #2, (**c**) #3, (**d**) #4, (**e**) #5, and (**f**) #6 in a groundwater matrix with an aquifer material loading of 100 g/L. Dash lines represent linear isotherm model fits.

Table 5. Linear isotherm fitting parameters and the corresponding K_d of PFAS adsorption onto aquifer materials.

		Aquifer Material					
		#1	**#2**	**#3**	**#4**	**#5**	**#6**
PFBS	K (L/g)	0.0006	0.0006	0.0008	0.0009	0.0007	0.0049
	R^2	0.92	0.92	0.99	0.93	0.99	0.98
	K_d (L/kg)	0.6	0.6	0.8	0.9	0.7	4.9
PFHpA	K (L/g)	0.0006	0.0009	0.0024	0.0042	0.0065	0.0303
	R^2	0.98	0.98	0.95	0.99	0.99	0.969
	K_d (L/kg)	0.6	0.9	2.4	4.2	6.5	30.3
PFOA	K (L/g)	0.0034	0.0056	0.0118	0.0276	0.0498	0.1379
	R^2	0.98	0.99	0.93	0.99	0.99	0.99
	K_d (L/kg)	3.4	5.6	11.8	27.6	49.8	137.9
PFHxS	K (L/g)	0.0037	0.0028	0.0174	0.0245	0.0289	0.1367
	R^2	0.97	0.99	0.90	0.98	0.99	0.99
	K_d (L/kg)	3.7	2.8	17.4	24.5	28.9	136.7
PFNA	K (L/g)	0.0117	0.0155	0.0356	0.1241	0.2597	0.3246
	R^2	0.97	0.98	0.94	0.99	0.99	0.99
	K_d (L/kg)	11.7	15.5	35.6	124.1	259.7	324.6
PFOS	K (L/g)	0.0245	0.0151	0.1401	0.3573	0.5678	1.1284
	R^2	0.96	0.99	0.93	0.99	0.99	0.99
	K_d (L/kg)	24.5	15.1	140.1	357.3	567.8	1128.4

In general, K_d represents the adsorption affinity between PFAS and a solid matrix. In the present work, K_d values were substantially varied for different aquifer materials, suggesting that PFAS adsorption was affected by aquifer material composition and structure. We performed a Pearson correlation analysis between K_d and various parameters of aquifer materials. For a given PFAS, we found that K_d was strongly positively related to the dolomite content of aquifer materials, and materials with higher dolomite contents exhibited much stronger affinity with PFAS (**Table 6** and **Figure 4**). For instance, compared to aquifer material #1, the K_d value of PFOS with aquifer material #6 consisting of predominantly dolomite increased by over 40 folds. In contrast, parameters such as porosity, CEC, and AEC had weak to negligible correlation with PFAS adsorption. Interestingly, it appeared that the contents of Si, Al, and Fe were negatively correlated with PFAS adsorption (**Table 6**). Increase of Si, Al, and Fe contents would reduce the content of dolomite, and thus reduce the adsorption affinity with PFAS.

Table 6. Pearson correlation coefficient (r) of *log* K_d of PFAS with various parameters of aquifer materials.

	dolomite wt%	Al wt%	Fe wt%	Silica wt%	porosity	CEC	AEC
PFBS	0.78	-0.87	-0.95	-0.74	-0.09	-0.01	-0.12
PFHpA	0.97	-0.96	-0.75	-0.99	-0.25	0.27	0.29
PFHxS	0.92	-0.98	-0.75	-0.89	-0.70	0.11	0.32
PFNA	0.97	-0.86	-0.50	-0.97	-0.88	0.45	0.54
PFOA	0.99	-0.93	-0.66	-0.98	-0.27	0.38	0.39
PFOS	0.91	-0.91	-0.57	-0.90	-0.24	0.23	0.50

A range of K_d values have been reported for PFAS adsorption onto natural materials, which have been related to different material compositions and properties, as well as the various experimental conditions. The K_d values obtained in the present work were generally higher than many of those reported for natural minerals [33, 46, 47]. For instance, although aquifer material #1 predominantly consisted of quartz, its K_d value with PFOS was much higher than those reported for Ottawa sand [48]. The higher K_d value obtained in this project may be related to the low PFAS concentrations used in the isotherm experiments. It has been suggested that K_d values between PFAS and adsorbent may depend on PFAS concentrations. Because of the abundance of surface sites, PFAS would prefer to occupy the high-energy strong adsorption sites when their concentrations were low. With the increase of PFAS concentrations, they started to occupy the low-energy weak adsorption sites, causing a reduction of K_d values [49]. Additionally, the minor content of dolomite in aquifer material #1 may also contribute to the higher K_d value than Ottawa sand. Overall, our results suggested that dolomite may have strong affinity with PFAS and play an important role in PFAS adsorption onto aquifer materials.

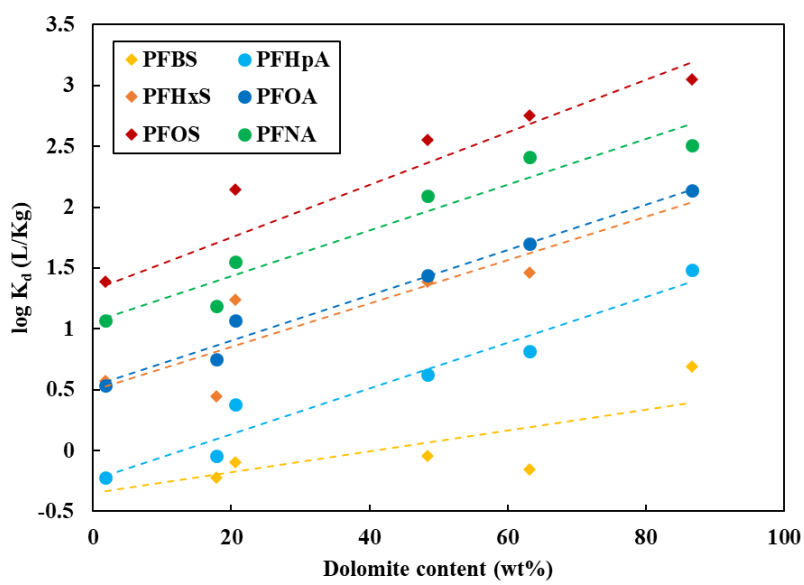

Figure 4. Correlation of *log* K_d of PFAS with dolomite contents of aquifer materials.

For a given aquifer material, the K_d values were strongly related to the PFAS structure. For PFAS with the same end functional group, the K_d values increased with increasing chain length of the perfluoroalkyl moiety (i.e., PFNA > PFOA > PFHpA, PFOS > PFHxS > PFBS). For PFAS with the same perfluoroalkyl moiety, the K_d values of sulfonic acids were higher than those of carboxylic acids (i.e., PFOS > PFNA, PFHxS > PFHpA). The octanol-water distribution coefficient (D_{ow}) is an important parameter for ionizable organic compounds. Compared to the octanol-water partition coefficient (K_{ow}), D_{ow} describes the ratio between the organic concentration in octanol and the organic concentration in water with the consideration of the neutral and all ionized species. Since the examined PFAS are present as anions under the experimental condition, D_{ow} may be more suitable than K_{ow} to represent PFAS properties in aqueous solution. Because of the wide range of *log* D_{ow} values reported in different literature, we used the *log* D_{ow} values of the examined PFAS from a single source for estimation. As shown in **Figure 5**, *log* K_d exhibited a good linear relationship with the *log* D_{ow} (at pH 8.5) of PFAS for all aquifer materials. Results suggested that *log* D_{ow} may be used as a general indicator to describe the adsorption of anionic PFAAs onto aquifer materials.

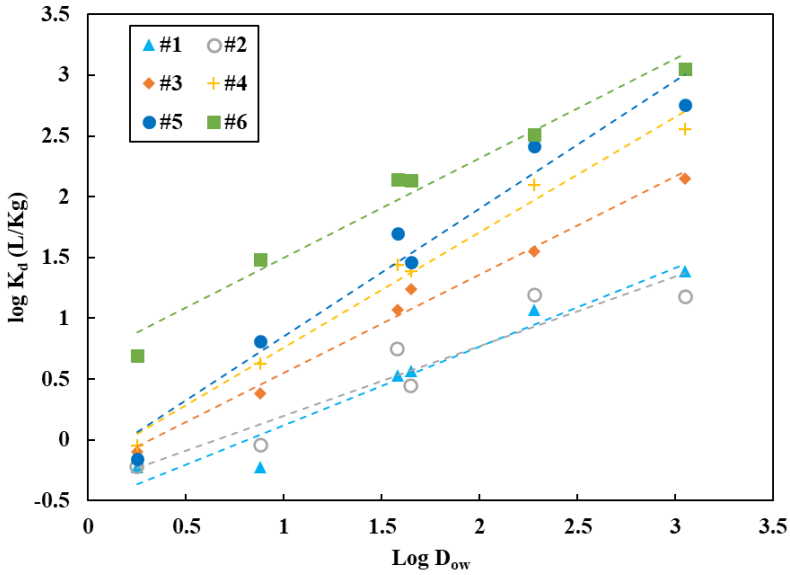

Figure 5. Correlation of *log* K_d of PFAS for each aquifer material with *log* D_{ow} of PFAS at pH 8.5.

Considering both the aquifer material composition and PFAS structure, we developed a simple multilinear regression model to estimate *log* K_d based on the dolomite content ($C_{dolomite}$) of aquifer materials and *log* D_{ow} of PFAS (Equation 11).

$$\log K_d = 1.68 \cdot C_{dolomite} + 0.81 \cdot \log D_{ow} - 0.81 \quad (11)$$

The model fitted the experimentally measured *log* K_d of PFAS quite well with a R^2 value of 0.92. **Figure 6** showed the comparison between the model calculated *log* K_d and measured *log* K_d. In general, the data points fell closely along the 1:1 line, suggesting that the multilinear regression model may be used to estimate the adsorption affinity of various PFAAs onto aquifer materials with varied contents of dolomite.

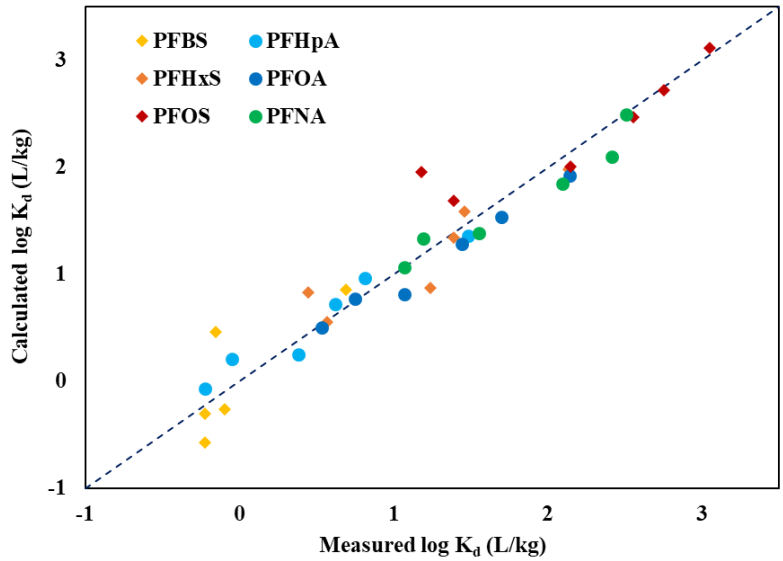

Figure 6. Relationship between measured *log* K_d with calculated *log* K_d from the multilinear regression model. The 1:1 line (dash line) is shown for reference.

Implications on PFAS transport in groundwater

Adsorption onto aquifer materials is an important process that affects the retardation and transport of PFAS in groundwater aquifer. To illustrate the impact of adsorption, we applied the measured K_d values to a 1-D model to simulate the transport behavior of PFAS through aquifers consisting of the six tested aquifer materials, with the assumption of continuous release of PFAS from the source (Equation 8). Both molecular diffusion and mechanical dispersivity could lead to the spread of chemicals within the subsurface, but these two processes could not generally be separated. Thus, the hydrodynamic dispersion coefficient (D) in Equation 8 was estimated by the following expression:

$$D=aLv+D^* \quad (12)$$

where aL (m) is the dynamic dispersivity and was estimated as ~4.42 m for a domain of 100 m [50]; v is the groundwater velocity and a representative value of ~10^{-6} m/s (~0.09 m/d) was used; and D^* (m^2/s) is the molecular diffusion coefficient. For PFAAs such as PFOA and PFOS, the measured values of D^* ranged from 0.45-2.5 × 10^{-9} m^2/s [51], which were several orders of magnitude lower than the mechanical dispersivity and could be reasonably ignored. The retardation factors (R) were calculated (**Table 7**) based on the K_d values of PFAS in Table 5 and aquifer material properties in Table 3.

Based on Equation 8 and the related estimated parameters, we calculated the concentration profile of the six PFAAs after 1 year of transport within aquifers consisting of the six aquifer materials (**Figure 7**). Clearly, PFAS transport was strongly related to the composition of aquifer materials, and aquifer materials with higher dolomite contents showed stronger retardation on PFAS transport. For comparison purpose, we selected $C_0/2$ (i.e., half of the source concentration) and calculated the corresponding PFAS travel distance. The travel distance of a given PFAS substantially decreased for aquifer materials with higher dolomite contents. For instance, compared to aquifer material #1, the travel distance of PFOS decreased by over six folds in aquifer

material #6. Meanwhile, shorter chain PFAS transported much faster than longer chain PFAS. For example, although aquifer material #6 showed highest retardation on PFAS transport, the travel distance of PFBS was over one order of magnitude higher than that of PFOS in aquifer material #6. It should be acknowledged that PFAS transport behavior in the field would be more complex and can be affected by factors such as media heterogeneity, diffusion to solid matrix, and dilution effect. Nevertheless, the 1-D transport model provided a quantitative illustration of the importance of aquifer material adsorption on PFAS transport.

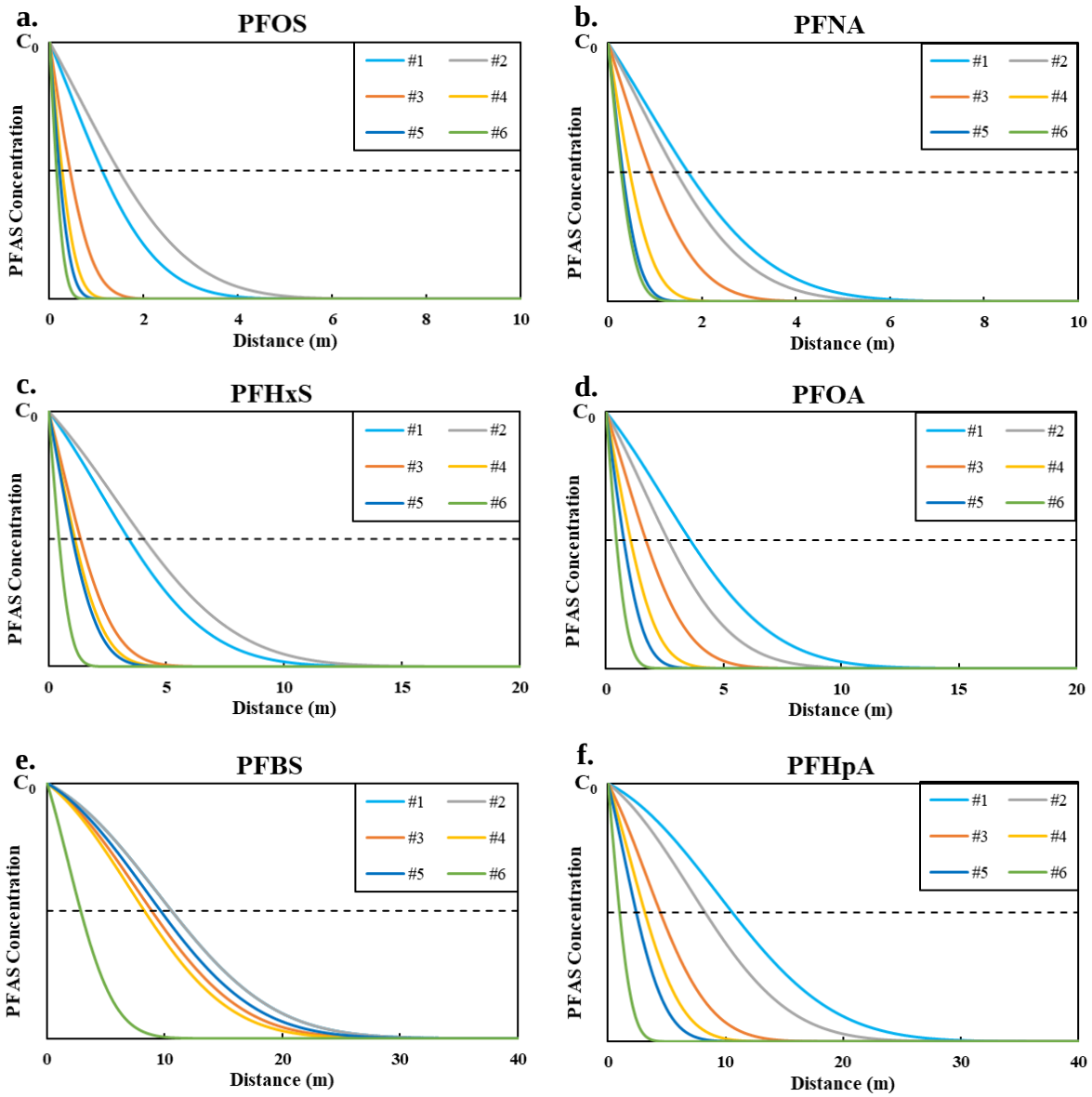

Figure 7. Calculated concentration profile of (**a**) PFOS, (b) PFNA, (**c**) PFHxS, (**d**) PFOA, (**e**) PFBS, and (**f**) PFHpA after 1 year of transport within aquifers consisting of the six aquifer materials based on 1-D transport model. The dash line in each panel represents $C_0/2$ line.

Table 7. Retardation factors (R) of PFAS within different aquifer materials.

Retardation Factor (R)	Aquifer Material					
	#1	#2	#3	#4	#5	#6
PFBS	4.0	4.2	5.0	4.6	6.0	29.8
PFHpA	4.0	5.8	13.0	18.0	47.0	179.0
PFOA	18.1	30.7	60.0	112.8	353.3	811.2
PFHxS	19.6	15.8	88.0	100.2	205.4	804.1
PFNA	59.9	83.2	179.0	503.6	1838.1	1908.0
PFOS	124.2	81.1	701.5	1448.1	4017.7	6630.4

Conclusions and Implications

This project presented a detailed investigation of the adsorption behavior of selected PFAS onto aquifer materials collected from various sites in Wisconsin. Aquifer material-water partition coefficients (i.e., K_d) of PFAS were determined for the first time under environmentally relevant PFAS concentrations and groundwater matrix. Several main conclusions were obtained.

- PFAS adsorption was highly dependent on aquifer material composition, particularly dolomite content. Aquifer materials of higher dolomite content showed significantly stronger affinity with PFAS than those of low dolomite content. Compared to dolomite content, other parameters of aquifer material such as contents of SiO_2, Al, and Fe, CEC, AEC, and porosity played a less substantial role in PFAS adsorption.

- PFAS adsorption was strongly related to PFAS structure. Overall, longer-chain PFAS had higher adsorption affinity with aquifer materials than those of shorter-chain PFAS, and perfluorinated sulfonic acids were more strongly adsorbed onto aquifer materials than perfluorinated carboxylic acids. Octanol-water distribution coefficient (i.e., D_{ow}) could be considered a good indicator to correlate PFAS structure with their adsorption onto aquifer materials.

- An empirical model was established based on multilinear regression of the experimental data to determine $log\ K_d$ of PFAS onto aquifer materials based on dolomite content of aquifer material and $log\ D_{ow}$ of PFAS. The empirical model may be used to provide a quick estimate of PFAS adsorption affinity and corresponding retardation factor in an impacted groundwater aquifer.

About two thirds of the people living in Wisconsin rely on groundwater as the primary source of drinking water. The occurrence of persistent PFAS in groundwater in Wisconsin represents a major growing public health concern. The transport and fate of PFAS within groundwater system is directly related to their adsorption onto aquifer materials which in turn is strongly dependent on the compositions and properties of aquifer materials. Findings from this project elucidated the

important role of dolomite on PFAS adsorption onto aquifer materials. The fundamental information of PFAS adsorption affinity obtained in this project may be used as a critical input parameter in the development of local and regional PFAS transport models, which would allow for the quantitative understanding of the fate and transport potential of PFAS in impacted groundwater aquifers in Wisconsin. It is worth mentioning that while this project primarily investigated the adsorption of six representative PFAS, the adsorption affinity of other relevant anionic PFAS onto aquifer materials may be estimated based on their $log\ D_{ow}$ values predicted by software (MarvinSketch). Overall, results of this project may be used to help the development of improved strategies for remediation of PFAS-contaminated sites, and guide general PFAS management practices in groundwater in Wisconsin.

We also recognize that within natural groundwater systems, PFAS can show complex transport behavior, and caution should be used when results from this project were to be extrapolated. For instance, although we believe that the fundamental chemical interactions between PFAS and dolomite, either in granular form or fractured form, would remain similar, it is highly likely that PFAS transport within fracture dolomite aquifer may be quite different due to differences in factors such as surface area, surface morphology and fluid flow paths in comparison to the granular media used in this project. To better understand PFAS adsorption and transport in various aquifer settings, we recommend future research efforts in the following directions: (1) determination of the impact of varied groundwater quality parameters on PFAS adsorption; (2) combined experimental and modeling activities to investigate PFAS adsorption and transport in complex aquifer systems such as fracture rock; and (3) elucidation of PFAS interaction mechanisms with aquifer materials through advanced computational and characterization tools.

References

[1] A.G. Paul, K.C. Jones, A.J. Sweetman, A first global production, emission, and environmental inventory for perfluorooctane sulfonate, Environmental science & technology 43 (2008) 386-392.

[2] S. KEMI, Occurrence and use of highly fluorinated substances and alternatives, Swedish Chemicals Agency Stockholm, Sweden, 2015.

[3] A.B. Lindstrom, M.J. Strynar, E.L. Libelo, Polyfluorinated Compounds: Past, Present, and Future, Environmental Science & Technology 45 (2011) 7954-7961.

[4] N. Merino, Y. Qu, R.A. Deeb, E.L. Hawley, M.R. Hoffmann, S. Mahendra, Degradation and removal methods for perfluoroalkyl and polyfluoroalkyl substances in water, Environmental Engineering Science 33 (2016) 615-649.

[5] Z. Wang, J.C. DeWitt, C.P. Higgins, I.T. Cousins, A Never-Ending Story of Per- and Polyfluoroalkyl Substances (PFASs)?, Environmental Science & Technology 51 (2017) 2508-2518.

[6] V. Barry, A. Winquist, K. Steenland, Perfluorooctanoic acid (PFOA) exposures and incident cancers among adults living near a chemical plant, Environmental health perspectives 121 (2013) 1313-1318.

[7] UNEP, The new POPs under the Stockholm Convention, 2019. http://www.pops.int/TheConvention/ThePOPs/TheNewPOPs/tabid/2511/Default.aspx

[8] J.L. Guelfo, D.T. Adamson, Evaluation of a national data set for insights into sources, composition, and concentrations of per-and polyfluoroalkyl substances (PFASs) in US drinking water, Environmental Pollution 236 (2018) 505-513.

[9] H.A. Kaboré, S.V. Duy, G. Munoz, L. Méité, M. Desrosiers, J. Liu, T.K. Sory, S. Sauvé, Worldwide drinking water occurrence and levels of newly-identified perfluoroalkyl and polyfluoroalkyl substances, Science of the Total Environment 616 (2018) 1089-1100.

[10] L. Gobelius, J. Hedlund, W. Dürig, R. Tröger, K. Lilja, K. Wiberg, L. Ahrens, Per-and polyfluoroalkyl substances in Swedish groundwater and surface water: implications for environmental quality standards and drinking water guidelines, Environmental science & technology 52 (2018) 4340-4349.

[11] X.C. Hu, D.Q. Andrews, A.B. Lindstrom, T.A. Bruton, L.A. Schaider, P. Grandjean, R. Lohmann, C.C. Carignan, A. Blum, S.A. Balan, Detection of poly-and perfluoroalkyl substances (PFASs) in US drinking water linked to industrial sites, military fire training areas, and wastewater treatment plants, Environmental science & technology letters 3 (2016) 344-350.

[12] USEPA, Fifth Unregulated Contaminant Monitoring Rule, 2021. https://www.epa.gov/dwucmr/fifth-unregulated-contaminant-monitoring-rule

[13] K. Hoffman, T.F. Webster, S.M. Bartell, M.G. Weisskopf, T. Fletcher, V.M. Vieira, Private drinking water wells as a source of exposure to perfluorooctanoic acid (PFOA) in communities surrounding a fluoropolymer production facility, Environmental health perspectives 119 (2010) 92-97.

[14] H.-M. Shin, V.M. Vieira, P.B. Ryan, R. Detwiler, B. Sanders, K. Steenland, S.M. Bartell, Environmental fate and transport modeling for perfluorooctanoic acid emitted from the

Washington Works Facility in West Virginia, Environmental science & technology 45 (2011) 1435-1442.

[15] J. Hatton, C. Holton, B. DiGuiseppi, Occurrence and behavior of per-and polyfluoroalkyl substances from aqueous film-forming foam in groundwater systems, Remediation Journal 28 (2018) 89-99.

[16] X. Dauchy, V. Boiteux, C. Bach, C. Rosin, J.-F. Munoz, Per-and polyfluoroalkyl substances in firefighting foam concentrates and water samples collected near sites impacted by the use of these foams, Chemosphere 183 (2017) 53-61.

[17] E.F. Houtz, C.P. Higgins, J.A. Field, D.L. Sedlak, Persistence of perfluoroalkyl acid precursors in AFFF-impacted groundwater and soil, Environmental science & technology 47 (2013) 8187-8195.

[18] S.A. Milley, I. Koch, P. Fortin, J. Archer, D. Reynolds, K.P. Weber, Estimating the number of airports potentially contaminated with perfluoroalkyl and polyfluoroalkyl substances from aqueous film forming foam: A Canadian example, Journal of environmental management 222 (2018) 122-131.

[19] E.F. Houtz, R. Sutton, J.-S. Park, M. Sedlak, Poly-and perfluoroalkyl substances in wastewater: Significance of unknown precursors, manufacturing shifts, and likely AFFF impacts, Water research 95 (2016) 142-149.

[20] J.R. Lang, B.M. Allred, J.A. Field, J.W. Levis, M.A. Barlaz, National estimate of per-and polyfluoroalkyl substance (PFAS) release to US municipal landfill leachate, Environmental science & technology 51 (2017) 2197-2205.

[21] H. Hamid, L.Y. Li, J.R. Grace, Review of the fate and transformation of per-and polyfluoroalkyl substances (PFASs) in landfills, Environmental pollution 235 (2018) 74-84.

[22] A. Blum, S.A. Balan, M. Scheringer, X. Trier, G. Goldenman, I.T. Cousins, M. Diamond, T. Fletcher, C. Higgins, A.E. Lindeman, The Madrid statement on poly-and perfluoroalkyl substances (PFASs), Environmental health perspectives 123 (2015) A107-A111.

[23] L. Schulte, Here's where testing has located PFAS or 'forever chemicals' in Wisconsin drinking water, Milwaukee Journal Sentinel (2022).

[24] L. Bergquist, Johnson Controls International takes $140 million charge for cleanup of 'forever' chemicals, Milwaukee Journal Sentinel (2019).

[25] M. McPherson, Contaminated drinking water at Milwaukee military base, 125 others, 2018. https://www.cbs58.com/news/contaminated-drinking-water-at-milwaukee-military-base-125-others

[26] J. Danbeck, Madison Water Utility finds PFAS in 4 more wells, bringing total to 14, 2019. https://www.nbc15.com/content/news/Madison-Water-Utility-finds-PFAS-in-4-more-wells-bringing-total-to-563335382.html

[27] J. Lu, La Crosse drinking water meets federal standards; unregulated contaminants present, La Crosse Tribune (2019).

[28] Wisconsin DHS, Chemicals: Perfluoroalkyl and Polyfluoroalkyl (PFAS) Substances, 2022. https://www.dhs.wisconsin.gov/chemical/pfas.htm

[29] Wisconsin DNR, New state maximum contaminant levels for drinking water, 2022. https://dnr.wisconsin.gov/topic/DrinkingWater/NR809.html

[30] C.Y. Tang, Q.S. Fu, D. Gao, C.S. Criddle, J.O. Leckie, Effect of solution chemistry on the adsorption of perfluorooctane sulfonate onto mineral surfaces, Water research 44 (2010) 2654-2662.

[31] J.L. Guelfo, C.P. Higgins, Subsurface transport potential of perfluoroalkyl acids at aqueous film-forming foam (AFFF)-impacted sites, Environmental science & technology 47 (2013) 4164-4171.

[32] A.V. Alves, M. Tsianou, P. Alexandridis, Fluorinated surfactant adsorption on mineral surfaces: implications for PFAS fate and transport in the environment, Surfaces 3 (2020) 516-566.

[33] Y. Li, D.P. Oliver, R.S. Kookana, A critical analysis of published data to discern the role of soil and sediment properties in determining sorption of per and polyfluoroalkyl substances (PFASs), Science of the Total Environment 628 (2018) 110-120.

[34] C.P. Higgins, R.G. Luthy, Sorption of perfluorinated surfactants on sediments, Environmental Science & Technology 40 (2006) 7251-7256.

[35] S. Mejia-Avendaño, G. Munoz, S. Sauvé, J. Liu, Assessment of the influence of soil characteristics and hydrocarbon fuel cocontamination on the solvent extraction of perfluoroalkyl and polyfluoroalkyl substances, Analytical chemistry 89 (2017) 2539-2546.

[36] G. Munoz, S.V. Duy, P. Labadie, F. Botta, H. Budzinski, F. Lestremau, J. Liu, S. Sauvé, Analysis of zwitterionic, cationic, and anionic poly-and perfluoroalkyl surfactants in sediments by liquid chromatography polarity-switching electrospray ionization coupled to high resolution mass spectrometry, Talanta 152 (2016) 447-456.

[37] USEPA, Hazardous waste test methods: SW–846, (1986).

[38] USEPA, Cation-exchange capacity of soils (sodium acetate), US EPA Washington, DC, USA, 1986.

[39] B.A. Schumacher, Methods for the determination of total organic carbon (TOC) in soils and sediments, (2002).

[40] M. Yamamuro, H. Kayanne, Rapid direct determination of organic carbon and nitrogen in carbonate-bearing sediments with a Yanaco MT-5 CHN analyzer, Limnology and Oceanography 40 (1995) 1001-1005.

[41] J.L. Schnoor, Environmental modeling: fate and transport of pollutants in water, air, and soil, John Wiley and Sons 1996.

[42] C.W. Fetter, Applied hydrogeology, Waveland Press 2018.

[43] J. Bertaux, F. Froehlich, P. Ildefonse, Multicomponent analysis of FTIR spectra; quantification of amorphous and crystallized mineral phases in synthetic and natural sediments, Journal of Sedimentary Research 68 (1998) 440-447.

[44] X. Liu, S.M. Colman, E.T. Brown, E.C. Minor, H. Li, Estimation of carbonate, total organic carbon, and biogenic silica content by FTIR and XRF techniques in lacustrine sediments, Journal of Paleolimnology 50 (2013) 387-398.

[45] S. Gunasekaran, G. Anbalagan, Thermal decomposition of natural dolomite, Bulletin of Materials Science 30 (2007) 339-344.

[46] A.C. Umeh, R. Naidu, S. Shilpi, E.B. Boateng, A. Rahman, I.T. Cousins, S. Chadalavada, D. Lamb, M. Bowman, Sorption of PFOS in 114 well-characterized tropical and temperate soils: Application of multivariate and artificial neural network analyses, Environmental Science & Technology 55 (2021) 1779-1789.

[47] F. Xiao, X. Zhang, L. Penn, J.S. Gulliver, M.F. Simcik, Effects of monovalent cations on the competitive adsorption of perfluoroalkyl acids by kaolinite: experimental studies and modeling, Environmental science & technology 45 (2011) 10028-10035.

[48] Y.H. Aly, C. Liu, D.P. McInnis, B.A. Lyon, J. Hatton, M. McCarty, W.A. Arnold, K.D. Pennell, M.F. Simcik, In situ remediation method for enhanced sorption of perfluoro-alkyl substances onto Ottawa sand, Journal of Environmental Engineering 144 (2018) 04018086.

[49] B. Yan, G. Munoz, S. Sauvé, J. Liu, Molecular mechanisms of per-and polyfluoroalkyl substances on a modified clay: a combined experimental and molecular simulation study, Water Research 184 (2020) 116166.

[50] M. Xu, Y. Eckstein, Use of weighted least-squares method in evaluation of the relationship between dispersivity and field scale, Groundwater 33 (1995) 905-908.

[51] C.E. Schaefer, D.M. Drennan, D.N. Tran, R. Garcia, E. Christie, C.P. Higgins, J.A. Field, Measurement of Aqueous Diffusivities for Perfluoroalkyl Acids, Journal of Environmental Engineering 145 (2019) 06019006.

Appendix

Details of PFAS analysis.

The analysis of the six PFAS mixture was performed on an ultra-high-performance liquid chromatograph (UHPLC, Shimadzu Nexera X2) coupled with ultra-fast triple quadrupole mass spectrometer (UFMS, Shimadzu LCMS-8060). An aliquot of the mass-labeled six PFAS mixture was added to the samples as internal standards. Chromatography was performed with a C18 column (Kinetex® 1.7 µm, 100 Å, 100 x 2.1 mm, Phenomenex). A delay column (Nexcol C18 5 µm, 3.0mm ID x 50 mm, Shimadzu) was placed in the mobile phase flow path before the sample injection valve to prevent contamination. The mobile phase consisted of (A) LCMS grade water with 20-mM ammonium acetate (Fisher Scientific) and (B) acetonitrile (Optima LCMS grade, Fisher Scientific) amended. Samples were injected at 50 µL volumes with a loading pump delivering at 400 µL/min of the mobile phase. The mobile phases gradient conditions were shown in **Table A1**. The column temperature was held constant at 40 ˚C.

MS/MS analysis was performed on the triple quadrupole UFMS with electrospray ionization operated in a negative mode. The operating parameters were set as nebulizing gas flow at 3 L/min, heating gas flow at 13 L/min, interface temperature at 300 °C, desolvation temperature at 526 °C, DL temperature at 100 °C, heat block temperature at 200 °C, and drying gas flow at 5 L/min. Nitrogen (>99.99% purity, Airgas) was used as the desolvation gas and nebulizing gas. LabSolutions V6.82 (Shimadzu) was used for instrument control, acquisition, and mass analysis. Matrix-matched calibration standards for the six PFAS mixture were used to minimize any matrix-induced effects, and PFAS concentrations were determined using the isotope dilution technique.

Table A1. Mobile phases gradient conditions for PFAS measurement in LC-UFMS.

Time (min)	% Mobile phase (A)	% Mobile phase (B)
0	90	10
2	70	30
9	45	55
11	20	80
13	20	80
14	90	10
15	90	10